

Electronic Supplementary Information

A zwitterionic chromophore as both biomarker-activatable optical imaging probe and therapeutic agent for detection and treatment of acute lung injury with bacterial infection

Zunpan She^a, Fang Zeng^{a,*}, Shuizhu Wu^{a,*}

^a Biomedical Division, State Key Laboratory of Luminescent Materials and Devices, Guangdong Provincial Key Laboratory of Luminescence from Molecular Aggregates, College of Materials Science and Engineering, South China University of Technology, Wushan Road 381, Guangzhou, 510640, China

Table of Contents

Experimental section.....	S3
Scheme S1.....	S8
Fig. S1.....	S9
Fig. S2.....	S9
Fig. S3.....	S10
Fig. S4.....	S10
Fig. S5.....	S11
Fig. S6.....	S11
Fig. S7.....	S12
Fig. S8.....	S12
Fig. S9.....	S13
Fig. S10.....	S13
Fig. S11.....	S14
Fig. S12.....	S14
Fig. S13.....	S15
Fig. S14.....	S15
Fig. S15.....	S15
Fig. S16.....	S16
Fig. S17.....	S16
Fig. S18.....	S17
Fig. S19.....	S17
Fig. S20.....	S18
Fig. S21.....	S18
Fig. S22.....	S19
Fig. S23.....	S19
Fig. S24.....	S20
Fig. S25.....	S20
Fig. S26.....	S21
Fig. S27.....	S21
Fig. S28.....	S22
Fig. S29.....	S22
Fig. S30.....	S23
References.....	S24

Experimental section

1. Reagents.

1,4-Butane sultone, 1,1,2-trimethylbenz[e]indole, phosphorus oxychloride, 4,4'-(propane-2,2-diyl) dicyclohexanone, sodium acetate, 2-amino-N,N,N-trimethylethanaminium chloride hydrochloride and triethylamine were purchased from Energy Chemical Reagents. The solvents including N, N-dimethylformamide (DMF) and dichloromethane (DCM) of analytical grade were dried with molecular sieve before use. Other solvents used in this study were analytical grade reagents and used without further purification. DMEM and 10% phosphate buffer saline (PBS) were purchased from KeyGen Bio-Tech. MAHMA NONOate (NO donor, also known as methylamine hexamethylene methylamine NONOate) was purchased from Cayman Chem. Gram-positive bacteria *Staphylococcus aureus* (*S. aureus*, ATCC 6538) was purchased from Biobw (Beijing, China). The Luria-Bertani (LB) medium and LB agar plates were supplied by Acme Biochemical Technology Co., Ltd. (Shanghai, China).

2. Apparatus.

Nuclear magnetic resonance (NMR) spectra were measured on Bruker AVANCE 400 MHz NMR spectrometer. ^1H NMR and ^{13}C NMR were conducted at 400 MHz and 101 MHz, respectively. High resolution mass spectrometer (MS) was recorded on a Bruker MAXIS IMPACT mass spectrometer. MALDI-TOF mass spectrometry was conducted with MALDI SYNAPT G2-Si High-Definition Mass Spectrometer. The Near-Infrared-II (NIR-II) fluorescence spectra were obtained on NIRQUEST512 spectrometer (excitation: 808 nm laser, emission range: 900-1700 nm). The absorption spectra were collected on Hitachi U-3010 spectrophotometer. The NIR-II fluorescence (in vivo and ex vivo) imaging was performed by using NIR-II in Vivo Fluorescent Imaging System (Series II 808/900-1700, Suzhou NIR-Optics Technologies Co., Ltd.). Optoacoustic imaging was performed using inVision128 multispectral optoacoustic tomographic (MSOT) imaging system (iThera Medical GmbH) equipped with viewMSOT 4.0 for data processing.

3. Syntheses

Synthesis of compounds 1 and 2: Compounds 1 and 2 was synthesized according to the reported method^[S1]. Briefly, Compound 1 was synthesized by reacting 1,4-butane sultone with 1,1,2-trimethyl-1H-benzo[e]indole in toluene. Compound 2 was prepared by reacting 4,4'-(Propane-2,2-diyl)dicyclohexanone with phosphorus oxychloride in DMF and dichloromethane.

Synthesis of compound 3: Under nitrogen atmosphere, Compound 1 (1.38 g, 4 mmol) and Compound 2 (384 mg, 1 mmol) were added to a single-neck round-bottom flask. Then acetic anhydride (5 mL) was added. Subsequently, sodium acetate (328 mg, 4 mmol) was added to the flask. The reaction mixture was stirred and heated to 80 °C for 2 h. After cooling to room temperature, the solvent was removed by evaporation under reduced pressure, and the residue was subjected to silica gel chromatography with $\text{CH}_2\text{Cl}_2/\text{CH}_3\text{OH}/\text{Et}_3\text{N}$ (41/8/1, v/v/v) as eluent to afford a green solid. Yield: 947 mg (56%). ^1H NMR (400 MHz, DMSO- d_6): δ 8.39

(d, $J = 13.9$ Hz, 4H), 8.25 (d, $J = 8.5$ Hz, 4H), 8.02 (t, $J = 6.2$ Hz, 8H), 7.80 (d, $J = 8.9$ Hz, 4H), 7.61 (t, $J = 7.4$ Hz, 4H), 7.48 (t, $J = 7.5$ Hz, 4H), 6.45 (d, $J = 14.0$ Hz, 4H), 4.38 (s, 8H), 2.59-2.50 (m, 8H), 1.91 (d, $J = 22.4$ Hz, 32H), 1.77 (s, 8H), 1.16 (t, $J = 7.2$ Hz, 16H). HR-MS (ESI) $[\text{C}_{95}\text{H}_{104}\text{Cl}_2\text{N}_4\text{O}_{12}\text{S}_4]^{2-}$ $[\text{M}]^{2-}$ m/z calcd 845.2956, found 845.2961.

Synthesis of ZW-N: Under nitrogen atmosphere, a mixture of Compound 3 (169 mg, 0.1 mmol) and 2-amino-N,N,N-trimethylethanaminium chloride hydrochloride (70 mg, 0.4 mmol) was dissolved in anhydrous DMF (5 mL). Subsequently, triethylamine (30 μL) was added to the solution. The mixture was stirred and heated to 70 $^\circ\text{C}$ for 4 h. After cooling to room temperature, the solvent was removed by evaporation under reduced pressure, and the residue was subjected to silica gel chromatography with $\text{CH}_2\text{Cl}_2/\text{CH}_3\text{OH}/\text{Et}_3\text{N}$ (30/19/1, v/v/v) as eluent to afford a deep red solid. Yield: 96 mg (52%). ^1H NMR (400 MHz, $\text{DMSO}-d_6$): δ 8.09 (d, $J = 6.3$ Hz, 4H), 7.91 (s, 8H), 7.75 (s, 4H), 7.53 (d, $J = 6.4$ Hz, 8H), 7.35 (s, 4H), 5.89 (s, 4H), 4.20 (s, 8H), 3.87 (s, 4H), 3.27 (s, 18H), 3.00 (s, 4H), 2.56 (s, 8H), 1.85 (d, $J = 12.4$ Hz, 34H), 1.74 (s, 8H), 1.23 (s, 4H), 1.14 (t, $J = 7.0$ Hz, 12H). ^{13}C NMR (126 MHz, $\text{CD}_3\text{OD}/\text{CDCl}_3$): δ 170.67, 140.14, 131.23, 130.17, 129.72, 128.27, 127.11, 123.89, 121.65, 120.68, 109.99, 94.66, 63.81, 63.04, 53.41, 50.52, 46.56, 43.15, 29.44, 27.61, 25.47, 22.26, 19.85, 8.16, 6.59. HR-MS (ESI) $[\text{C}_{105}\text{H}_{132}\text{N}_8\text{O}_{12}\text{S}_4 + \text{Na}]^+ [\text{M} + \text{Na}]^+ m/z$ calcd 1847.8745, found 1847.8740.

4. Measurement of optical spectra.

For measurement of NO response, MAHMA NONOate was used as the NO donor. The stock solution of the probe ZW-N was prepared in EtOH. After the addition of NO donor (final concentration 0-80 μM) into ZW-N solutions in PBS (10 mM, pH = 7.4), the test solutions (with ZW-N final concentration of 5.0 μM) were allowed to incubate for 1 min at 37 $^\circ\text{C}$, and then their absorption spectra and fluorescent spectra were recorded. In the time-dependent experiments, the spectra of the test solutions were recorded at different time periods after the probe's incubation with NO. In the selectivity-evaluation experiments, the spectra of test solutions were recorded at 1 min after adding NO donor or other substances. In stability studies, ZW-N was pretreated with MAHMA NONOate for 1 min to ensure complete reaction between the activatable probe and NO, and then the reaction product upon being exposed to continual irradiation by 808 nm laser (300 $\text{mW}\cdot\text{cm}^{-2}$) for a total period of 60 min, and their absorption spectra were recorded. In the experiments concerning optical-spectral stability under simulated physiological conditions, ZW-N test solutions was prepared in 10 mM DPBS + 1% Tween + 10% FBS, after the addition of NO donor, the test solutions were allowed to incubate for 1 min at 37 $^\circ\text{C}$, and their fluorescent spectra were recorded. The excitation light in the fluorescent spectra measurement was an 808 nm laser at a power density of 70 $\text{mW}\cdot\text{cm}^{-2}$.

5. Phantom optoacoustic imaging.

The test solutions containing 5 μM ZW-N in PBS (10 mM, pH = 7.4) and varied concentrations of MAHMA NONOate (0, 10, 20, 30, 40, 50, 60, 70 and 80 μM) were incubated for 1 min at 37 $^\circ\text{C}$. Then the solutions were added into commercial Wilmad NMR tubes for phantom optoacoustic imaging which was conducted with MSOT system. In selectivity-evaluation experiments, the spectra of test solutions were obtained at 1 min after

adding NO donor or other substances. The OA images were reconstructed at 850 nm with the back-projection reconstruction method.

6. Relative Optoacoustic (OA) intensity.

Relative OA intensity was calculated with the equation:

$$\text{Relative OA intensity} = [(OA_{850})_{\text{NO}} - (OA_{850})_{\text{control}}] / (OA_{850})_{\text{control}}$$

where $(OA_{850})_{\text{NO}}$ is the OA intensity at 850 nm of ZW-N in PBS treated with MAHMA NONOate, $(OA_{850})_{\text{control}}$ is the OA intensity at 850 nm of the control (PBS).

7. Cell experiments.

Mouse fibroblast cells (L929 cells) were obtained from Jiangsu KeyGEN BioTECH Co. Ltd. and cultured in Dulbecco's modified Eagle's medium (DMEM) containing 10% fetal bovine serum (FBS) and 1% penicillin and streptomycin at 37 °C with 5% CO₂ humidified atmosphere.

Methyl thiazolyl tetrazolium (MTT) assay was conducted to investigate the in vitro cytotoxicity of the probe ZW-N. First, L929 cells were inoculated into 96-well plates at a cell density of 5000 cells/well and grown for 24 h. Then, the medium in each well was discarded, and the cells were washed with PBS three times and then incubated with fresh medium containing different concentrations (0, 5, 10, 20, 40 and 80 μM) of the probe ZW-N for another 48 hours. Next, each well was washed with PBS and the cells were allowed to grow in the medium containing 0.5 mg·mL⁻¹ MTT for 2 h. And then, the culture medium containing MTT was discarded, and DMSO (150 μL) was added into each well to dissolve the precipitates. Finally, the absorbance at 570 nm for each well was recorded by Thermo MK3 ELISA reader to reflect the cell viability. In this experiment, 3 independent experiments were repeated and 8 replicates were measured for each concentration of the probe. The statistical mean and standard deviation were employed to estimate cell viabilities.

8. Protein adsorption assay.

The compound ZW-N or ZW-N + NO and BSA or HAS were mixed in 3 mL PBS (final ZW-N or ZW-N + NO concentration: 1 mg·mL⁻¹, final BSA or HAS concentration: 2 mg·mL⁻¹) and shaken at 37 °C for 1 h. The mixtures were centrifuged and the supernatants were collected for measuring the characteristic UV absorbance at 280 nm. The BSA or HSA concentrations in supernatants were determined using the calibration curves obtained from BSA or HAS of known concentrations. The protein adsorption was calculated according to the equation:

$$\text{Protein adsorption} = (C_0V_0 - C_xV_x) / W$$

where C_0 is the initial BSA or HSA concentrations; C_x is the BSA or HSA concentrations in the supernatants; V_0 is the initial the volume of the mixed solutions; V_x is the volume of the supernatants; W is the initial weight of the compound ZW-N (3 mg) or ZW-N + NO (3 mg).

9. Animal studies.

Specific-pathogen-free (SPF) male BALB/c mice (6-7 weeks old) were provided by Guangdong Medical Laboratory Animal Center and kindly kept in the Laboratory Animal Center of South China Agricultural University. All mice had ad libitum access to SPF diet and

sterile water and kept under a 12 h light/dark cycle. Mice housing and all in vivo experiments were approved by the Ethics Committee of Laboratory Animal Center from South China Agricultural University (Approval No. 2023-D046) and performed following the institution's regulations as well as in accordance with the Regulations on the Management of Laboratory Animals of China. Before imaging experiments, depilation was conducted for the mice using a commercial depilatory agent. In imaging experiments, mice were randomly divided into 3 mice in each group.

10. In vivo imaging for LPS-induced ALI model mice.

Mice were treated with lipopolysaccharide (LPS, 5 mg·kg⁻¹ body weight, 40 μL, intratracheal administration) for 24 h to establish mice models with ALI as the model group. LPS-induced ALI model mice received treatment with NAC (400 mg/kg, i.p.) at two dosages (0 and 12 h) at different time points as the treatment group. Healthy mice receiving intratracheal administration of saline (40 μL) were chosen as the control group. There were three mice per group.

After different groups of mice were anesthetized with 2% isoflurane in oxygen, and then underwent intratracheal administration of ZW-N (0.05 mg·kg⁻¹) for fluorescence imaging in vivo. The fluorescence images were taken with the NIR-II in-Vivo Imaging System (excitation: 808 nm laser with 50 mW·cm⁻², emission filter: 900-1700 nm). In addition, after different groups of mice were anesthetized with 2% isoflurane in oxygen, and placed in the animal holder for optoacoustic imaging at several time periods after intratracheal administration with the probe. The following wavelengths were selected based on the major turning points in the absorption spectra of ZW-NO, Hb and HbO₂: 680 nm, 700 nm, 730 nm, 760 nm, 780 nm, 800 nm, 835 nm, 850 nm, 875 nm and 900 nm (background). 10 individual frames at each wavelength were recorded. Cross-sectional images were acquired with a step size of 0.5 mm spanning through the whole scanning region.

11. In vivo imaging for LPS-induced ALI mice with bacterial infection (*S. aureus* infection).

Mice were treated with LPS (5 mg·kg⁻¹ body weight, 40 μL, intratracheal administration) for 24 h and then treated with *S. aureus* (10⁷ CFU·mL⁻¹, 20 μL, intratracheal administration) for 6 h to establish the ALI with bacterial infection mouse model (referred to as the LPS + Bacteria group). The ALI with bacterial infection model mice underwent treatment with NAC (400 mg/kg, i.p.) of two dosages (at 6 and 12 h) are referred to as the LPS + Bacteria & NAC group. The ALI with bacterial infection model mice underwent treatment with NAC (400 mg/kg, i.p.) and ZW-N (0.05 mg·kg⁻¹) with intratracheal administration of two dosages (at 6 and 12 h) are referred to as the LPS + Bacteria & NAC + ZW-N group. Healthy mice receiving intratracheal administration of saline (40 μL) were chosen as the control group. There were three mice per group.

After different groups of mice were anesthetized with 2% isoflurane in oxygen and underwent intratracheal administration with ZW-N (0.05 mg·kg⁻¹) for NIR-II fluorescence imaging in vivo. The fluorescence images were taken with the NIR-II in-Vivo Imaging System (excitation: 808 nm laser with 50 mW·cm⁻², emission filter: 900-1700 nm). In addition, after different groups of mice were anesthetized with 2% isoflurane in oxygen, and

placed in the animal holder for optoacoustic imaging at several time periods after intratracheal administration with the probe. The following wavelengths were selected based on the major turning points in the absorption spectra of ZW-NO, Hb and HbO₂: 680 nm, 700 nm, 730 nm, 760 nm, 780 nm, 800 nm, 835 nm, 850 nm, 875 nm and 900 nm (background). 10 individual frames at each wavelength were recorded. Cross-sectional images were acquired with a step size of 0.5 mm spanning through the whole scanning region.

12. H&E staining analysis.

Organs were dissected and immersed in 10% formalin for 24 h. All the fixed organs were processed for paraffin embedding, sectioned, and stained with hematoxylin and eosin (H&E). For further biosafety assessment, healthy mice were *i.v.* injected daily with an equal volume of saline or the probe, and the major organs (including heart, liver, spleen, lung and kidney) were dissected and subjected to H&E staining at day 7 after saline or probe injection.

13. Analysis of mouse body weight.

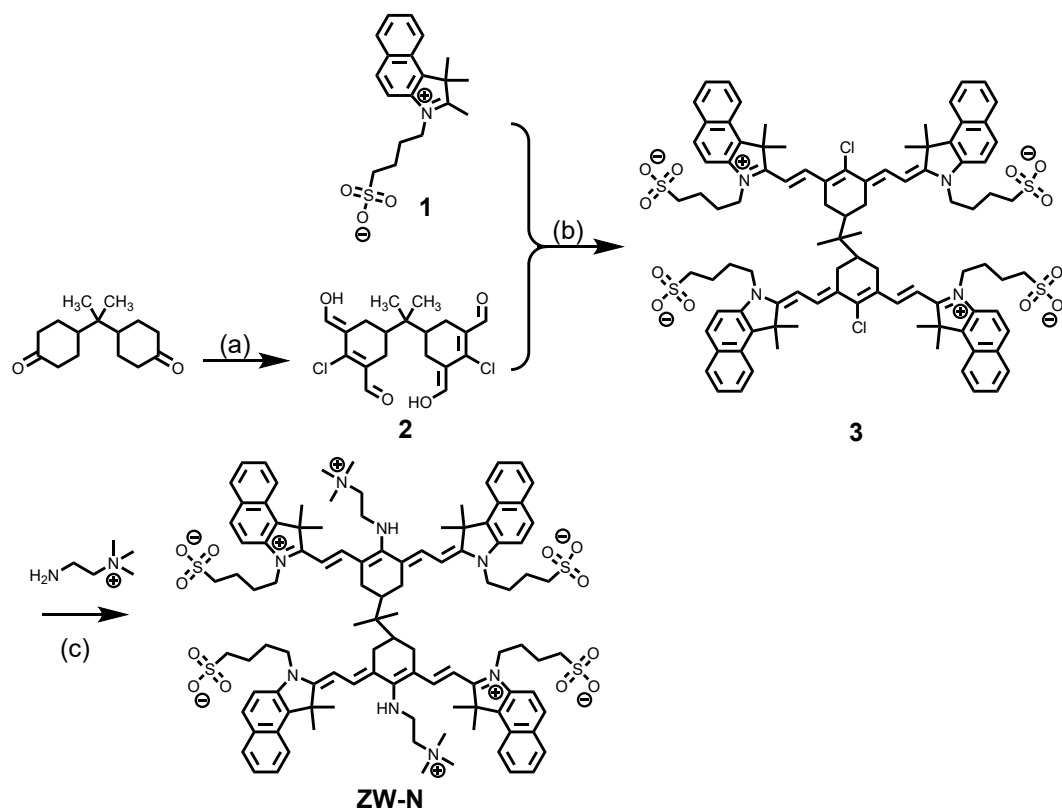
To study the effect of the probe ZW-N on the body weights of the mice, mice were treated with the probe (0.05 mg·kg⁻¹, in 40 µL saline) or an equal volume of saline (40 µL) by *i.v.* injection, and then the body weights of the mice were monitored for 7 days.

14. Bacteria Culture.

Staphylococcus aureus was initially stored at -80 °C. A small amount of *S. aureus* stock solution was transferred into 5 mL of liquid medium and incubated at 37 °C with shaking (170 rpm). The Luria-Bertani (LB) liquid medium was used for the culture of *S. aureus*.

To assess the bactericidal ability of the probe, different concentrations of the probe ZW-N were co-incubated with *S. aureus* in liquid medium for 24 h, then diluted separately and spread onto LB agar plates for evaluating the bacterial colonies.

For evaluation of bacterial burden of the lung, the lung tissue samples from the mice were homogenized and diluted with sterile PBS. The obtained tissue homogenate was diluted and spread onto LB agar plates (n = 3) for evaluating the bacterial colonies.



Scheme S1. Synthetic route for ZW-N.

Reagents, conditions and yields: a) POCl_3 , DMF, DCM, 0 °C, 1 h; 50 °C, 3 h; b) Acetic anhydride, sodium acetate, 80 °C, N_2 , 2 h; c) DMF, 2-amino-N,N,N-trimethylethanaminium chloride hydrochloride, triethylamine, 70 °C, N_2 , 4 h.

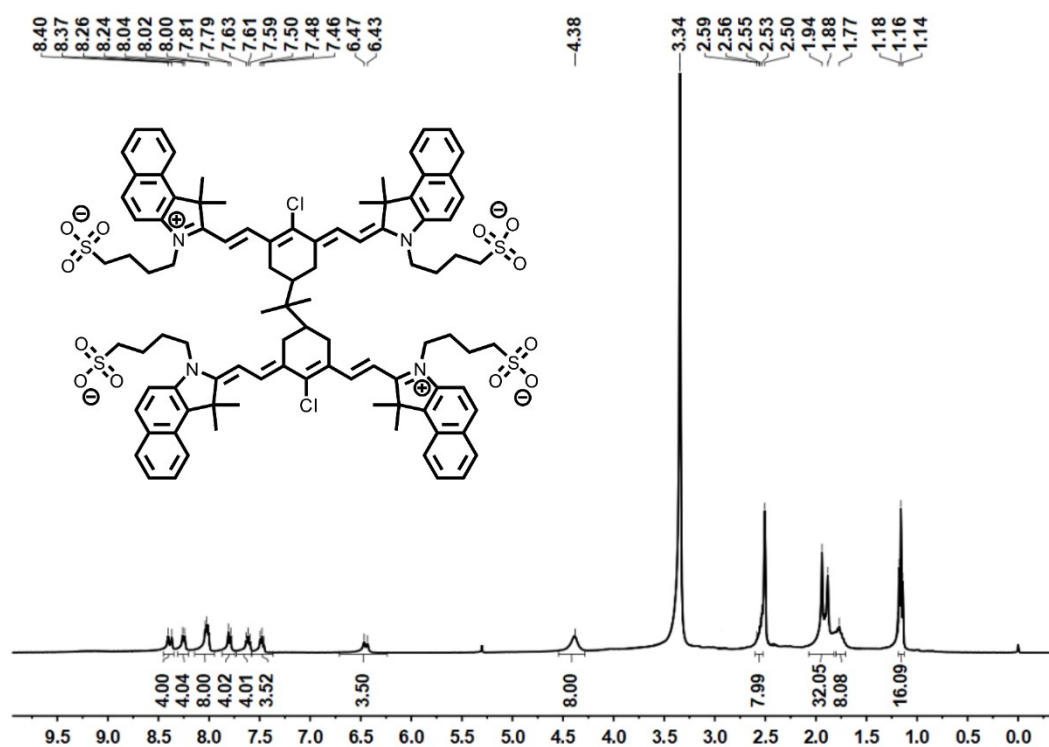


Fig. S1. ^1H NMR spectrum of compound 3 in $\text{DMSO-}d_6$.

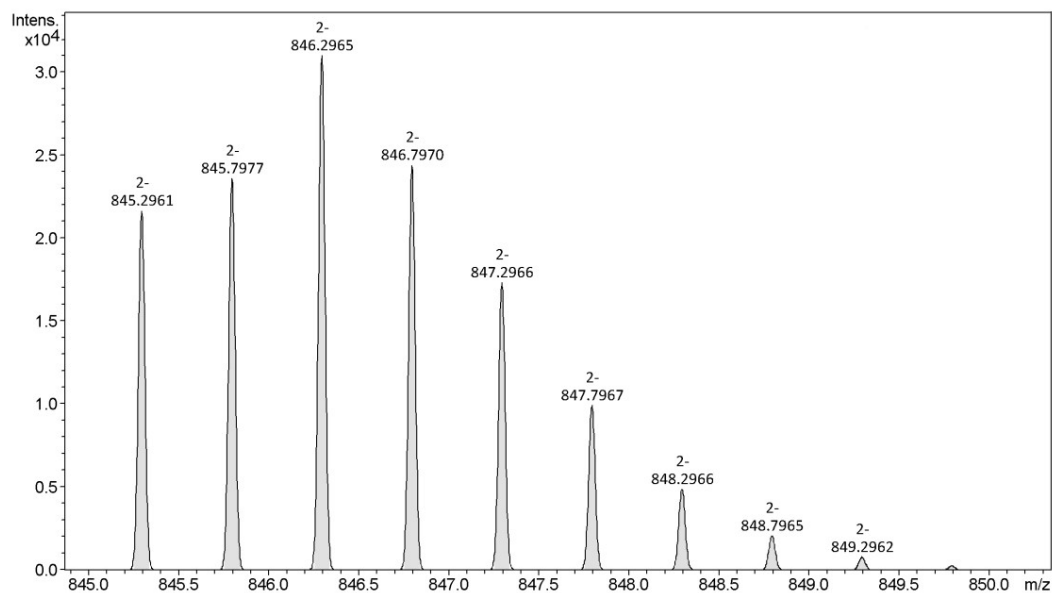


Fig. S2. HR Mass spectrum of compound 3.
 $[\text{M}]^{2-} [\text{C}_{95}\text{H}_{104}\text{Cl}_2\text{N}_4\text{O}_{12}\text{S}_4]^{2-}$ m/z 845.2961

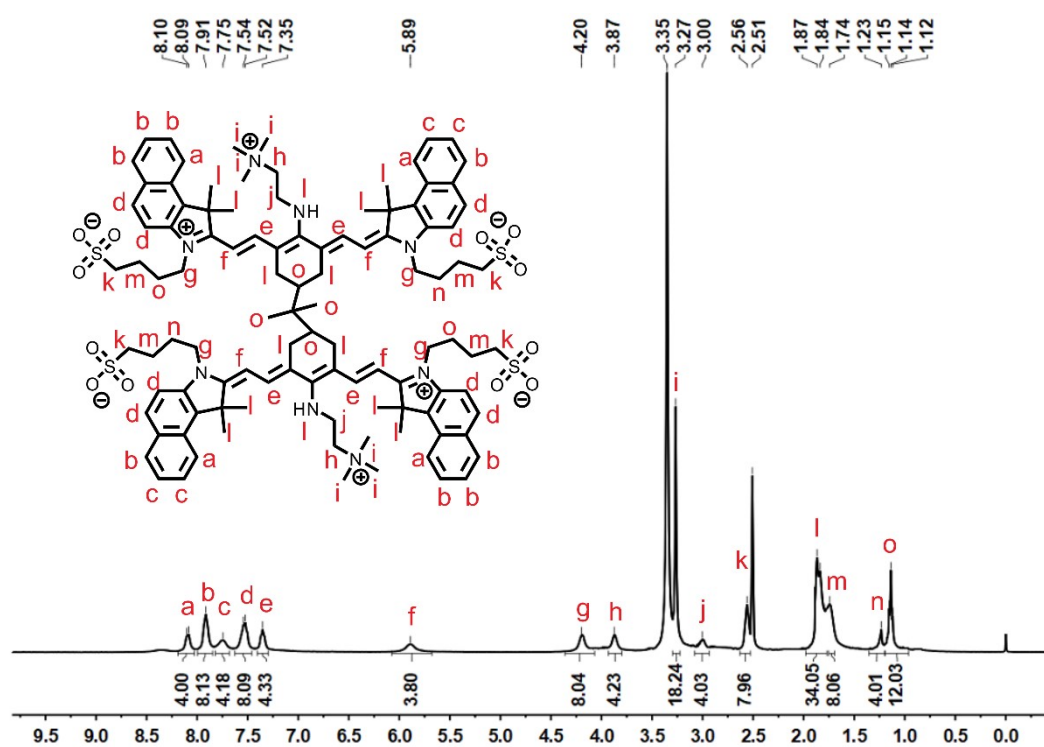


Fig. S3. ^1H NMR spectrum of ZW-N in $\text{DMSO}-d_6$.

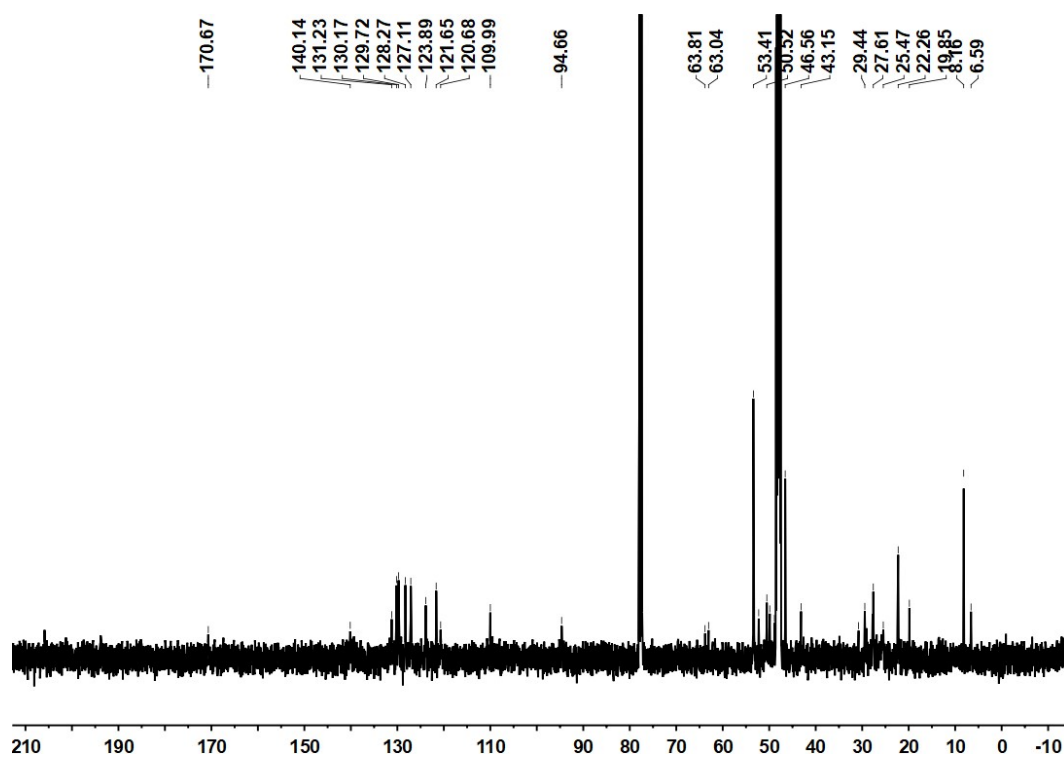


Fig. S4. ^{13}C NMR spectrum of ZW-N in $\text{CD}_3\text{OD}/\text{CDCl}_3$.

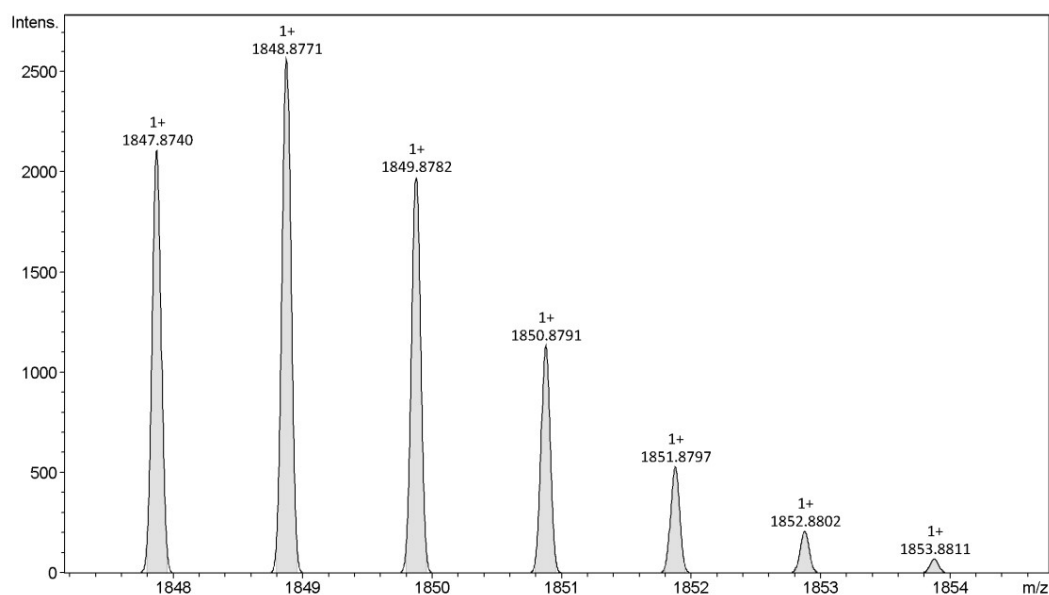


Fig. S5. HR Mass spectrum of ZW-N.

$[M + Na]^+ [C_{105}H_{132}N_8O_{12}S_4 + Na]^+ m/z 1847.8745$

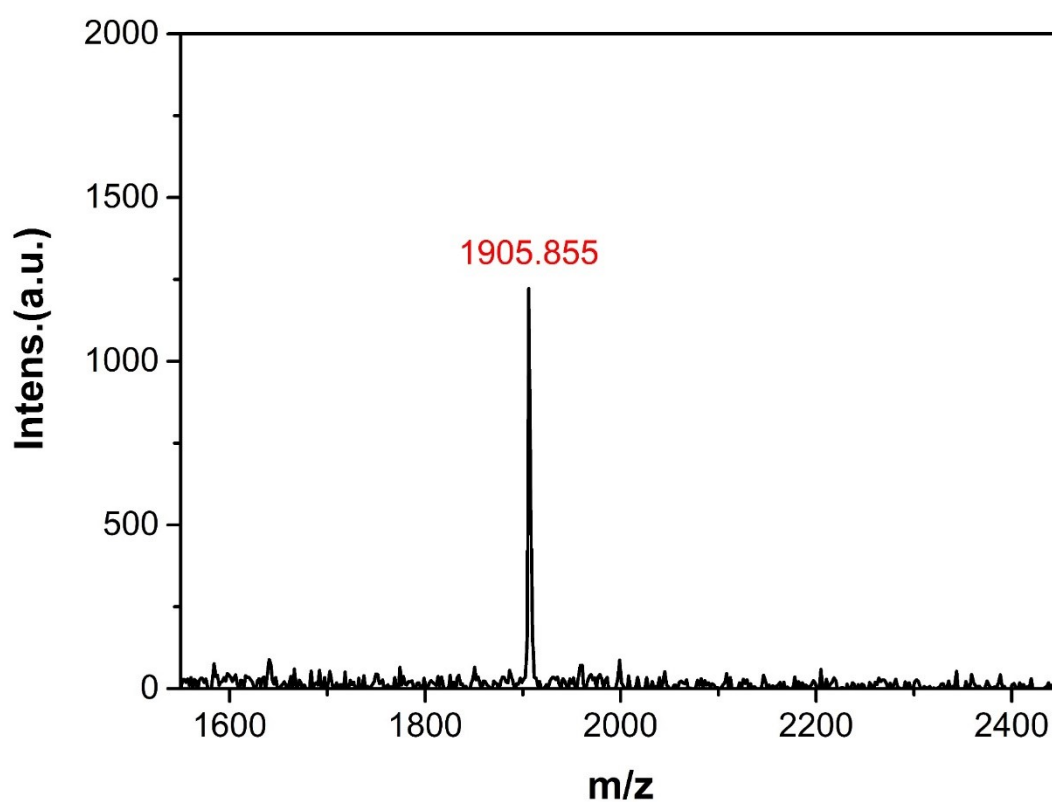


Fig. S6. MALDI-TOF mass spectrum of ZW-N after being incubated with NO donor (MAHMA NONOate) in PBS (10 mM, pH 7.4).

Response product (ZW-NO) m/z $[M + Na]^+ [C_{105}H_{130}N_{10}O_{14}S_4 + Na]^+ 1905.855$

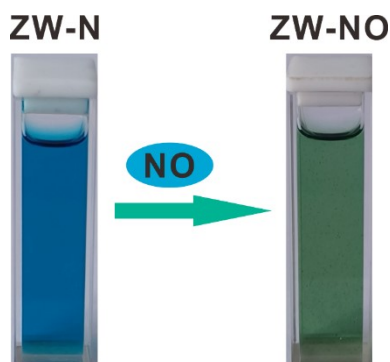


Fig. S7. Photographs of ZW-N solution before and after incubation with NO.

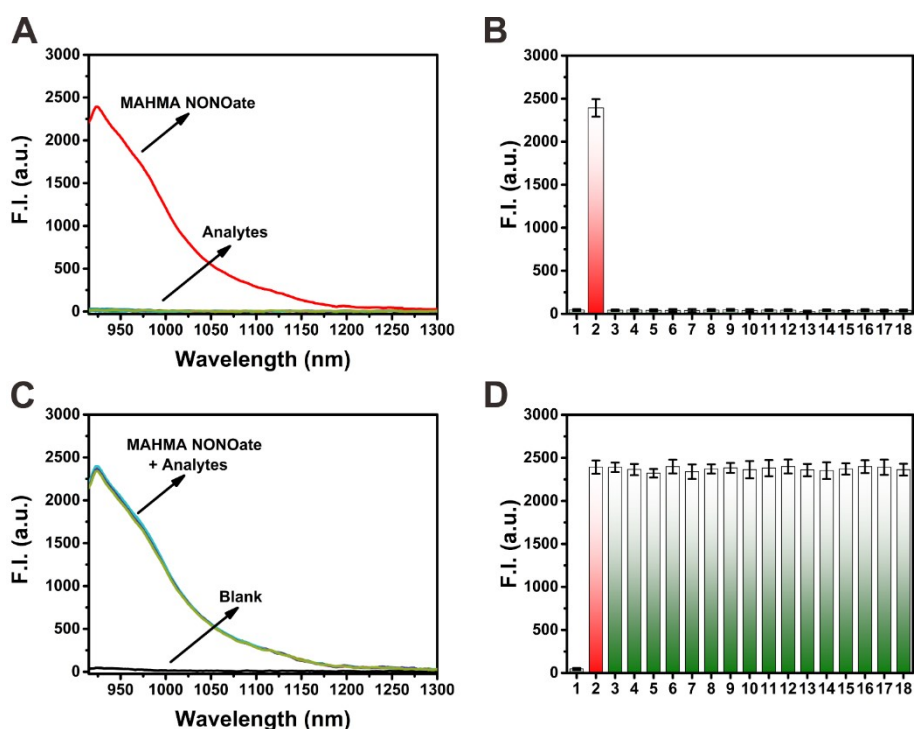


Fig. S8. (A) The fluorescence spectra of the probe ZW-N (5 μ M) upon incubation with different substances respectively in PBS (10 mM, pH = 7.4) at 37 $^{\circ}$ C for 1 min. (B) Fluorescent intensity at 924 nm of the probe ZW-N (5 μ M) upon incubation with different substances respectively in PBS (10 mM, pH = 7.4) at 37 $^{\circ}$ C for 1 min. (C) The fluorescence spectra of the probe ZW-N (5 μ M) upon treatment with 80 μ M MAHMA NONOate and simultaneously in the presence of individual substance respectively for 1 min in PBS (10 mM, pH 7.4) at 37 $^{\circ}$ C. (D) Fluorescent intensity at 924 nm of the probe ZW-N (5 μ M) upon treatment with 80 μ M MAHMA NONOate and simultaneously in the presence of individual substance respectively for 1 min in PBS (10 mM, pH 7.4) at 37 $^{\circ}$ C. Excitation laser: 808 nm. (1. Blank (probe solution only), 2. MAHMA NONOate (80 μ M), 3. H_2O_2 (100 μ M), 4. O_2^- (100 μ M), 5. ClO^- (100 μ M), 6. NO_2^- (100 μ M), 7. H_2S (100 μ M), 8. Cys (100 μ M), 9. GSH (1 mM), 10. Glu (1 mM), 11. Tyr (1 mM), 12. K^+ (1 mM), 13. Ca^+ (1 mM), 14. Na^+ (1 mM), 15. Cu^{2+} (1 mM), 16. I^- (1 mM), 17. Br^- (1 mM), 18. Cl^- (1 mM). (n = 3).

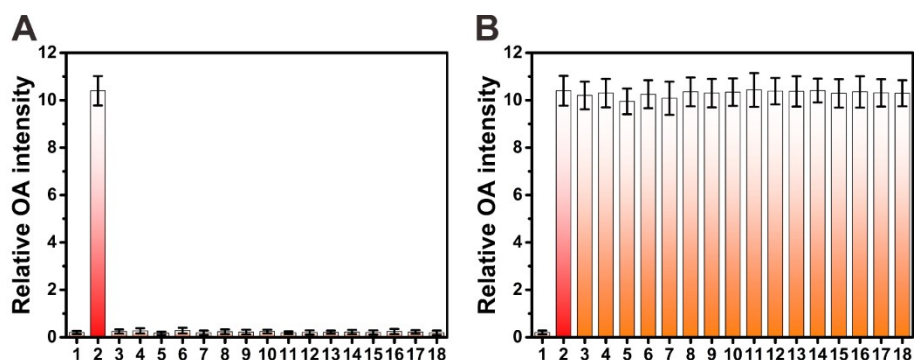


Fig. S9. (A) Relative optoacoustic intensity of the probe ZW-N (5 μ M) upon incubation with different substances respectively in PBS (10 mM, pH = 7.4) at 37 $^{\circ}$ C for 1 min. (B) Relative optoacoustic intensity the probe ZW-N (5 μ M) upon treatment with 80 μ M MAHMA NONOate and simultaneously in the presence of individual substance respectively for 1 min in PBS (10 mM, pH 7.4) at 37 $^{\circ}$ C. Excitation laser: 808 nm. (1. Blank (probe solution only), 2. MAHMA NONOate (80 μ M), 3. H_2O_2 (100 μ M), 4. O_2^- (100 μ M), 5. ClO^- (100 μ M), 6. NO_2^- (100 μ M), 7. H_2S (100 μ M), 8. Cys (100 μ M), 9. GSH (1 mM), 10. Glu (1 mM), 11. Tyr (1 mM), 12. K^+ (1 mM), 13. Ca^+ (1 mM), 14. Na^+ (1 mM), 15. Cu^{2+} (1 mM), 16. I^- (1 mM). 17. Br^- (1 mM), 18. Cl^- (1 mM). (n = 3).

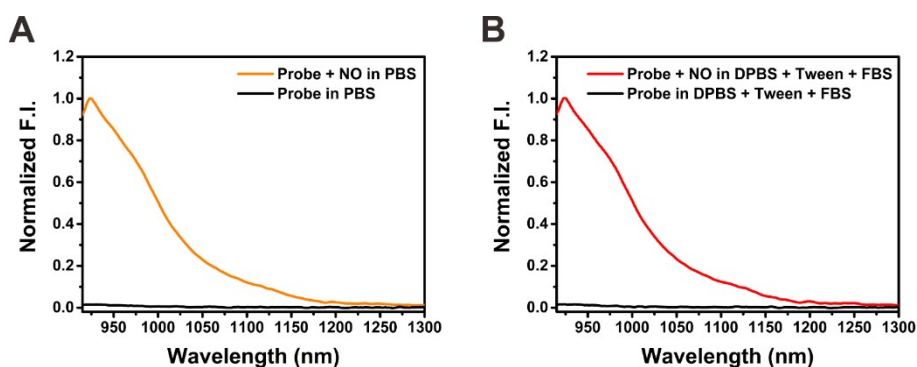


Fig. S10. (A) Normalized fluorescence spectra of the probe (5 μ M) and the probe (5 μ M) after being incubated with MAHMA NONOate in 10 mM PBS for 1 min at 37 $^{\circ}$ C. (B) Normalized fluorescence spectra of the probe (5 μ M) and the probe (5 μ M) after being incubated with MAHMA NONOate in 10 mM DPBS (Dulbecoo's phosphate buffered saline) + 1% Tween + 10% FBS (fetal bovine serum) for 1 min at 37 $^{\circ}$ C. Excitation laser: 808 nm.

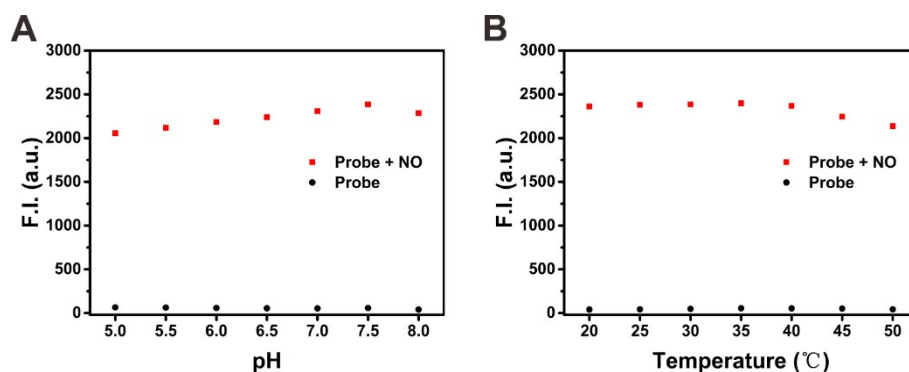


Fig. S11. (A) Fluorescent intensity at 924 nm of the probe ZW-N (5 μ M) in buffer solutions at different pH values at 37 $^{\circ}$ C for 1 min and the probe after being incubated with MAHMA NONOate in buffer solutions at different pH values. (B) Fluorescent intensity at 924 nm of the probe ZW-N (5 μ M) upon incubation with PBS at different temperatures for 1 min and the probe after being incubated with MAHMA NONOate in PBS at different temperatures. Excitation laser: 808 nm.

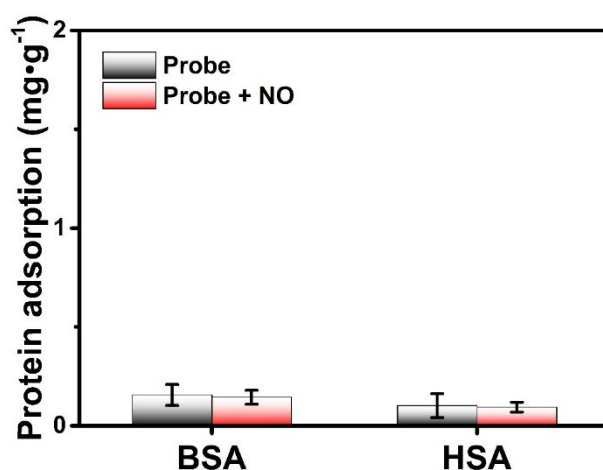


Fig. S12. Protein adsorption for the probe or the probe after being incubated with MAHMA NONOate in PBS with BSA or HSA (n = 3).

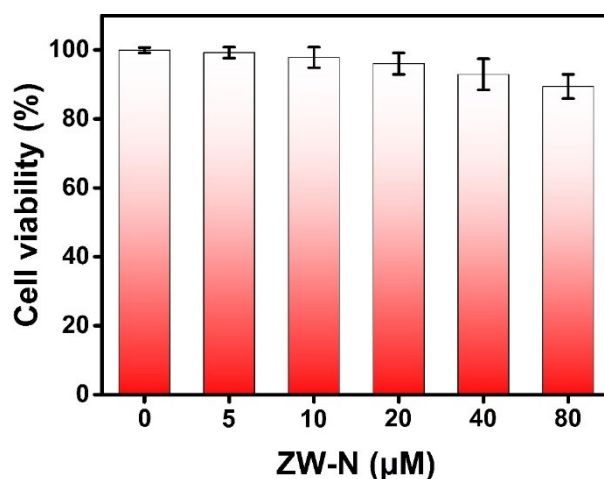


Fig. S13. Viabilities of L929 cells upon incubation with different concentrations (0, 5, 10, 20, 40 and 80 μM) of the probe ZW-N by MTT assay. Three independent experiments were conducted for each concentration and eight replicates were performed in each independent experiment. Data represent mean \pm SD. Error bars represent the standard deviation (SD).

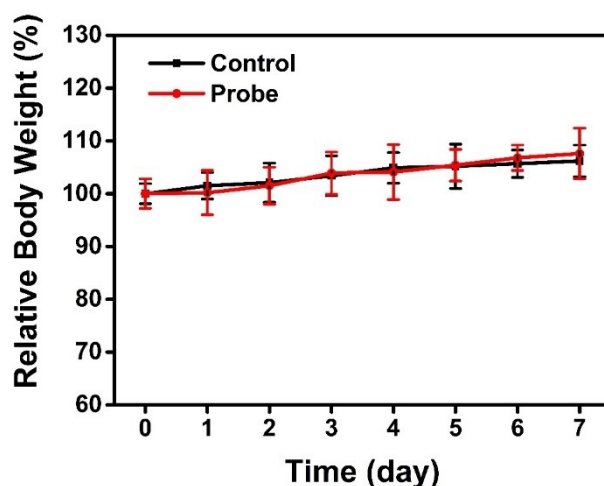


Fig. S14. Changes in relative body weights of healthy mice within 7d upon intravenously injected with saline (the control) or the probe ($0.05 \text{ mg}\cdot\text{kg}^{-1}$ in $40 \mu\text{L}$ saline) daily. ($n = 3$).

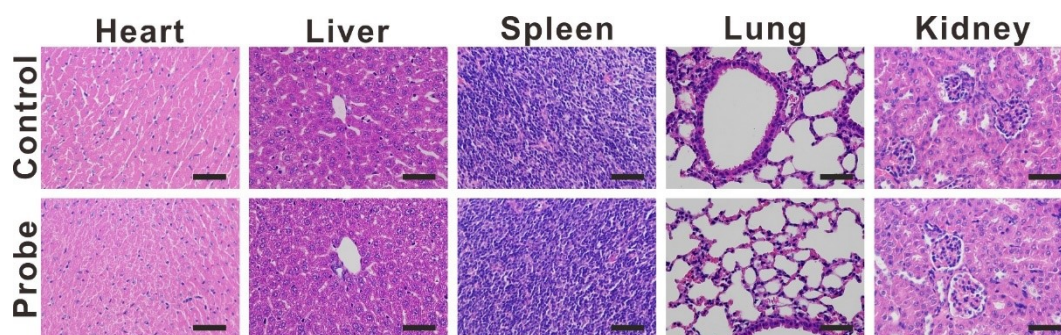


Fig. S15. H&E staining analyses of the tissue sections of heart, liver, spleen, lung and kidney from healthy the mice at 7d after *i.v.* injection of saline or the probe ZW-N (0.05 mg kg^{-1} , in $40 \mu\text{L}$ saline). Scale bar = $50 \mu\text{m}$.

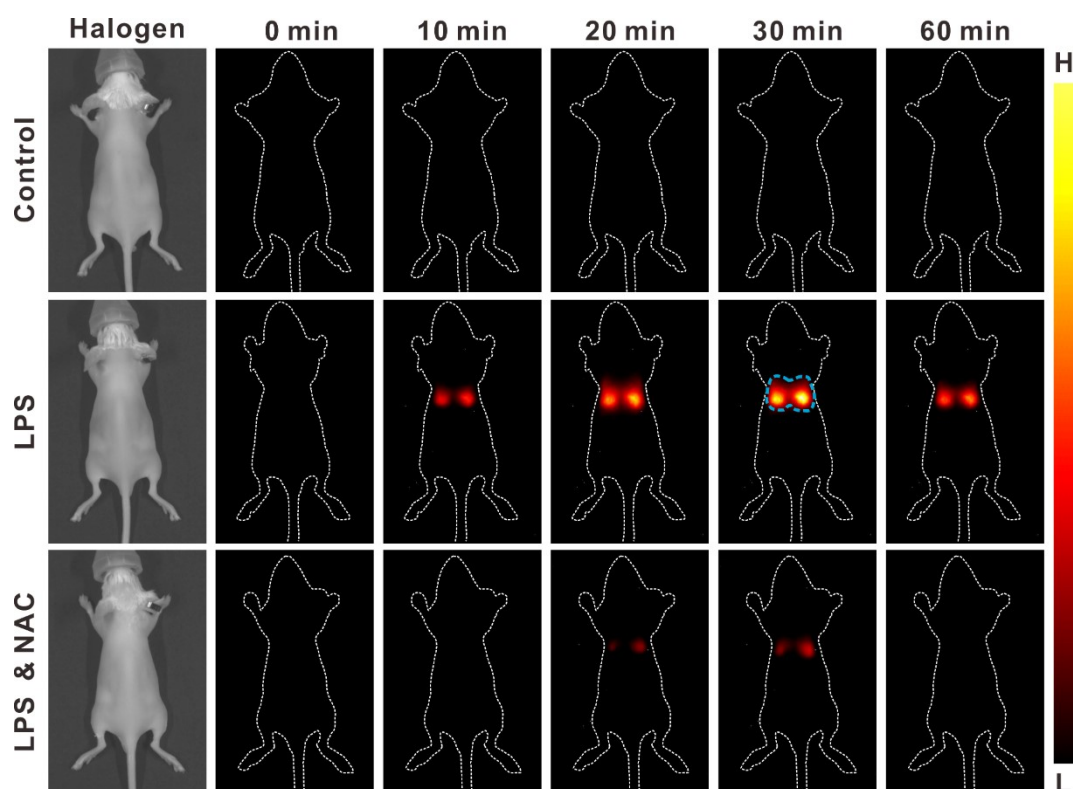


Fig. S16. Fluorescence images of the mice from different groups at different time periods after intratracheal administration of ZW-N ($0.05 \text{ mg} \cdot \text{kg}^{-1}$, in saline). The mice were in prone posture. Blue dotted circles: the ROI covering the lungs. Excitation laser: 808 nm , power density: $50 \text{ mW} \cdot \text{cm}^{-2}$.

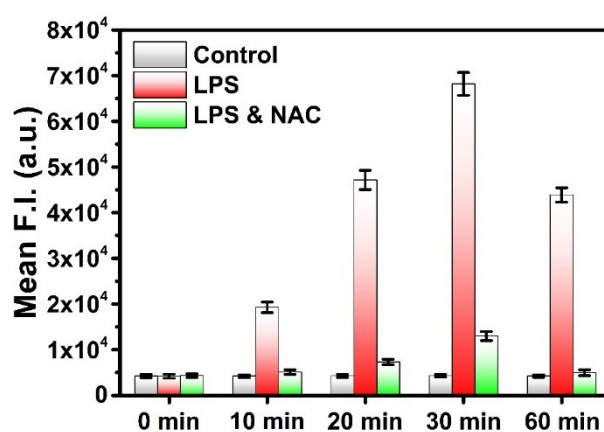


Fig. S17. Mean fluorescent intensities at the ROI covering the lungs (Blue dotted circles) displayed in Fig. S16 ($n = 3$). Data with error bars represent the mean plus/minus SD.

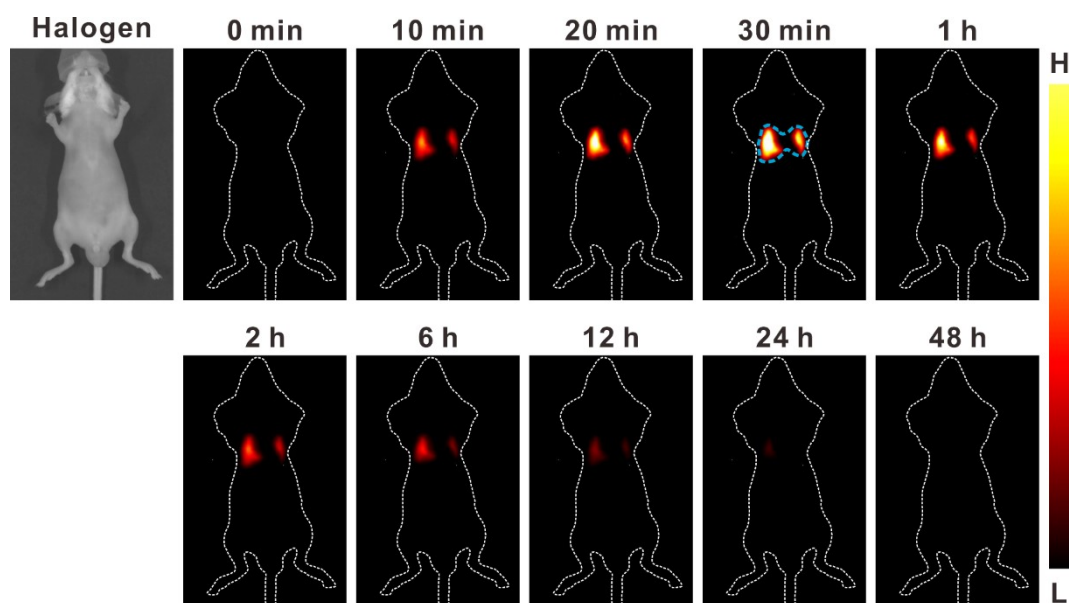


Fig. S18. Fluorescence images of the mice within 48 h upon intratracheal administration of the probe after being incubated with MAHMA NONOate. The mice were in supine posture. Blue dotted circles: the ROI covering the lungs. Excitation laser: 808 nm, power density: 50 mW·cm⁻².

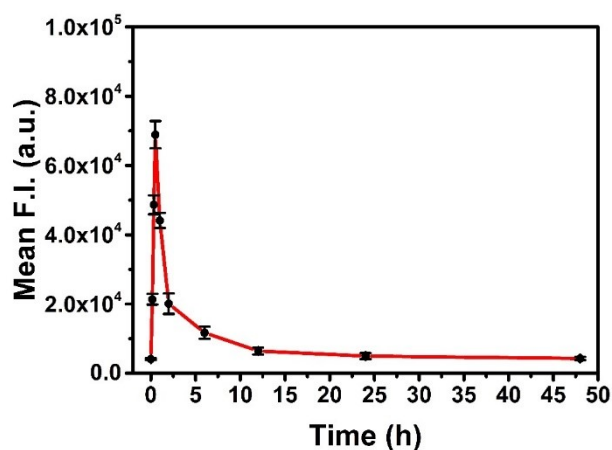


Fig. S19. Mean fluorescence intensity at the lung region (blue dotted circles) displayed in Fig. S18. (n = 3).

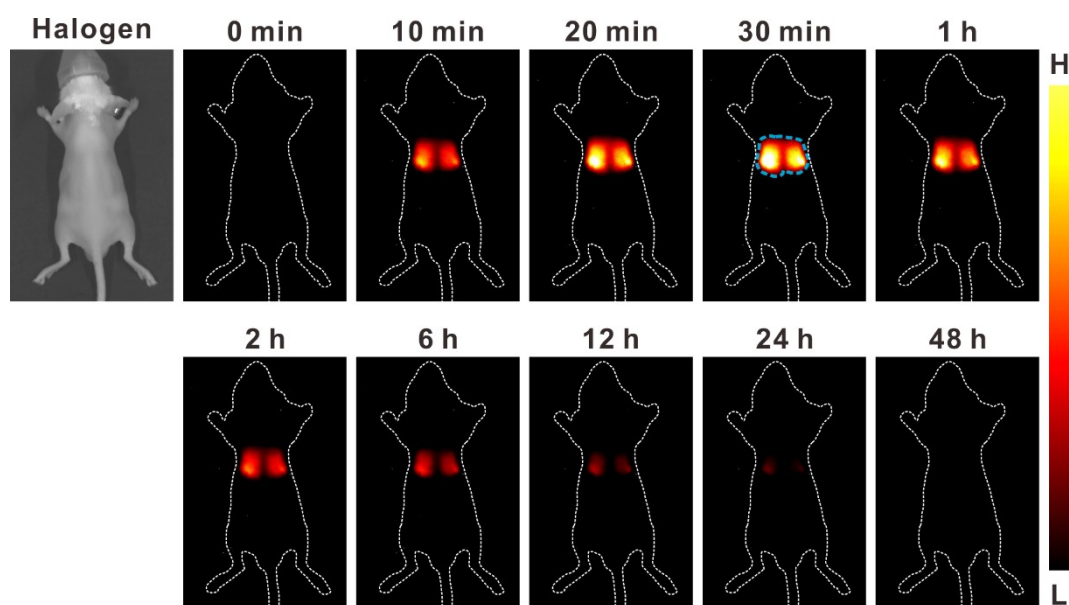


Fig. S20. Fluorescence images of the mice within 48 h after intratracheal administration of the probe after being incubated with MAHMA NONOate. The mice were in prone posture. Blue dotted circles: the ROI covering the lungs. Excitation laser: 808 nm, power density: 50 mW·cm⁻².

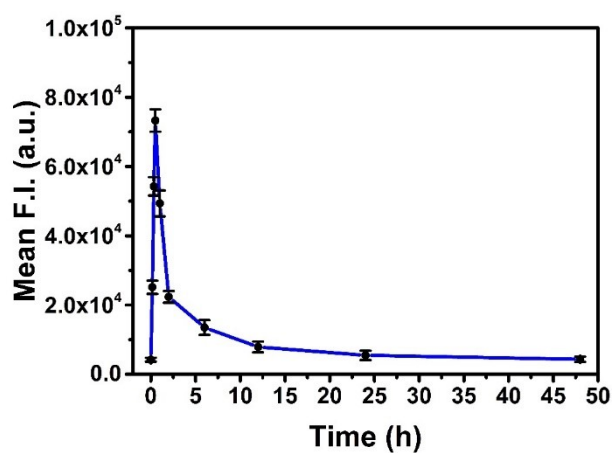


Fig. S21. Mean fluorescence intensity at the lung region (blue dotted circles) displayed in Fig. S20. (n = 3).

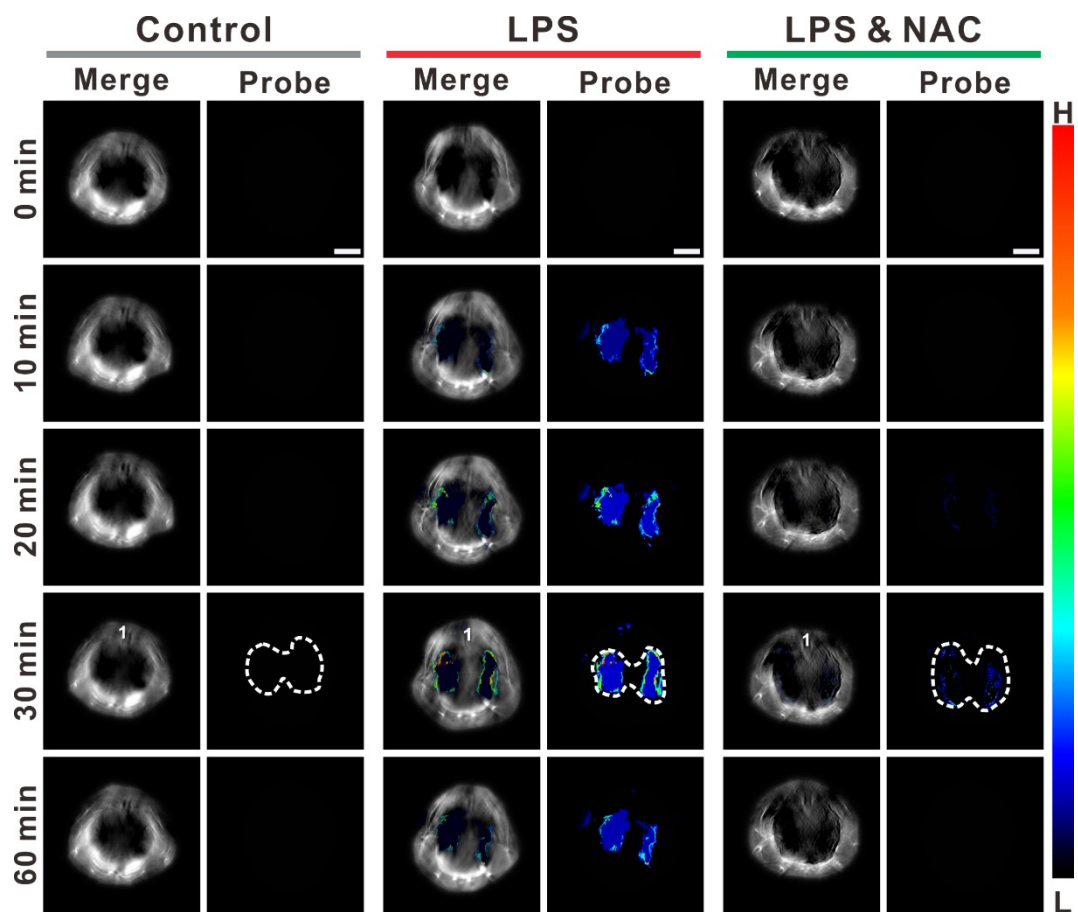


Fig. S22. Cross-sectional MSOT images of the mice from different groups at different time points after intratracheal administration of ZW-N ($0.05 \text{ mg} \cdot \text{kg}^{-1}$, in saline). Left: Overlay of the optoacoustic signals of the activated probe with the grayscale background image. Right: the optoacoustic signals of the activated probe. “1” indicates spinal cord. The mice were in prone posture. White dotted circle indicates the ROI covering the lungs. Scalebar: 5 mm.

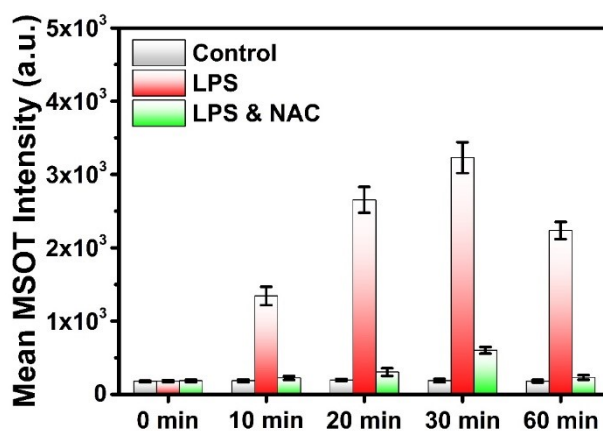


Fig. S23. Mean MSOT intensities of the ROI covering the lungs (white dotted circle) displayed in Fig. S22 ($n = 3$). Data with error bars represent the mean plus/minus SD.

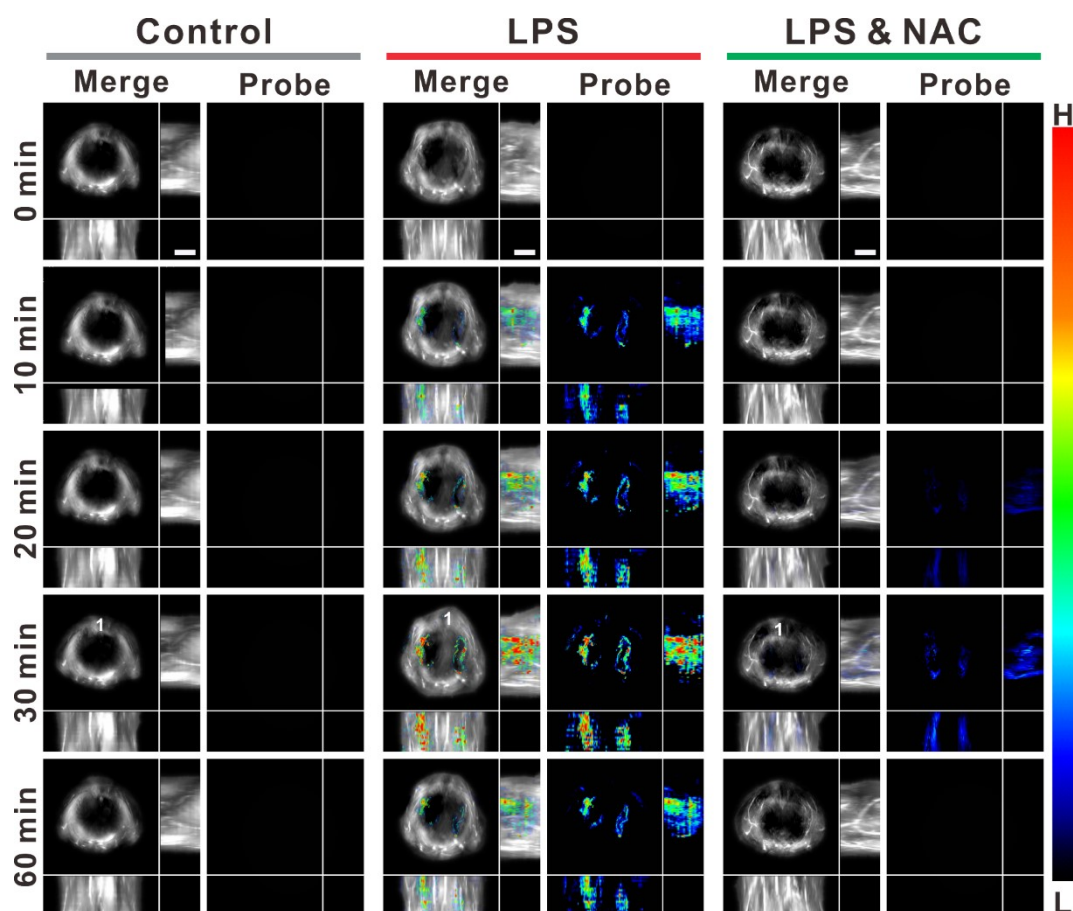


Fig. S24. 3D-MSOT images of the mice from different groups at different time points after intratracheal administration of ZW-N ($0.05 \text{ mg} \cdot \text{kg}^{-1}$, in saline). Left: Overlay of the optoacoustic signals of the activated probe with the grayscale background image. Right: The optoacoustic signals of the activated probe. “1” indicates spinal cord. The mice were in prone posture. Scalebar: 5 mm.

For the 3D MSOT images, the top-left subpanel represents the x-y plane, the top-right subpanel represents the y-z plane, and the bottom-left subpanel represents the x-z plane.

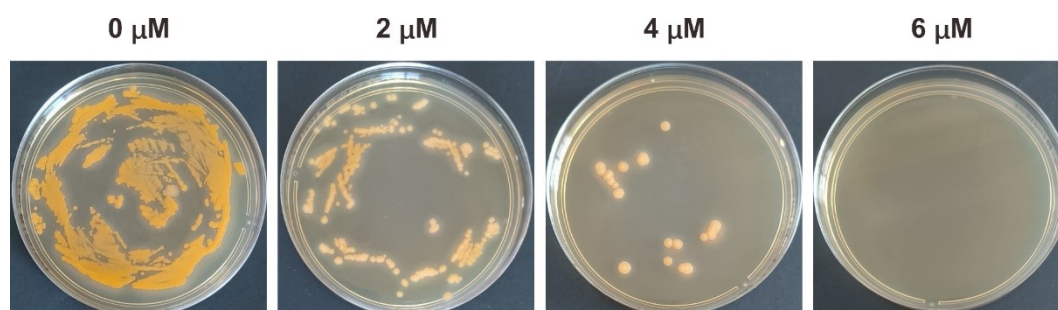


Fig. S25. Bacterial colonies observation on the agar plates after bacteria (*S. aureus*) incubation with different concentrations of probe ZW-N.

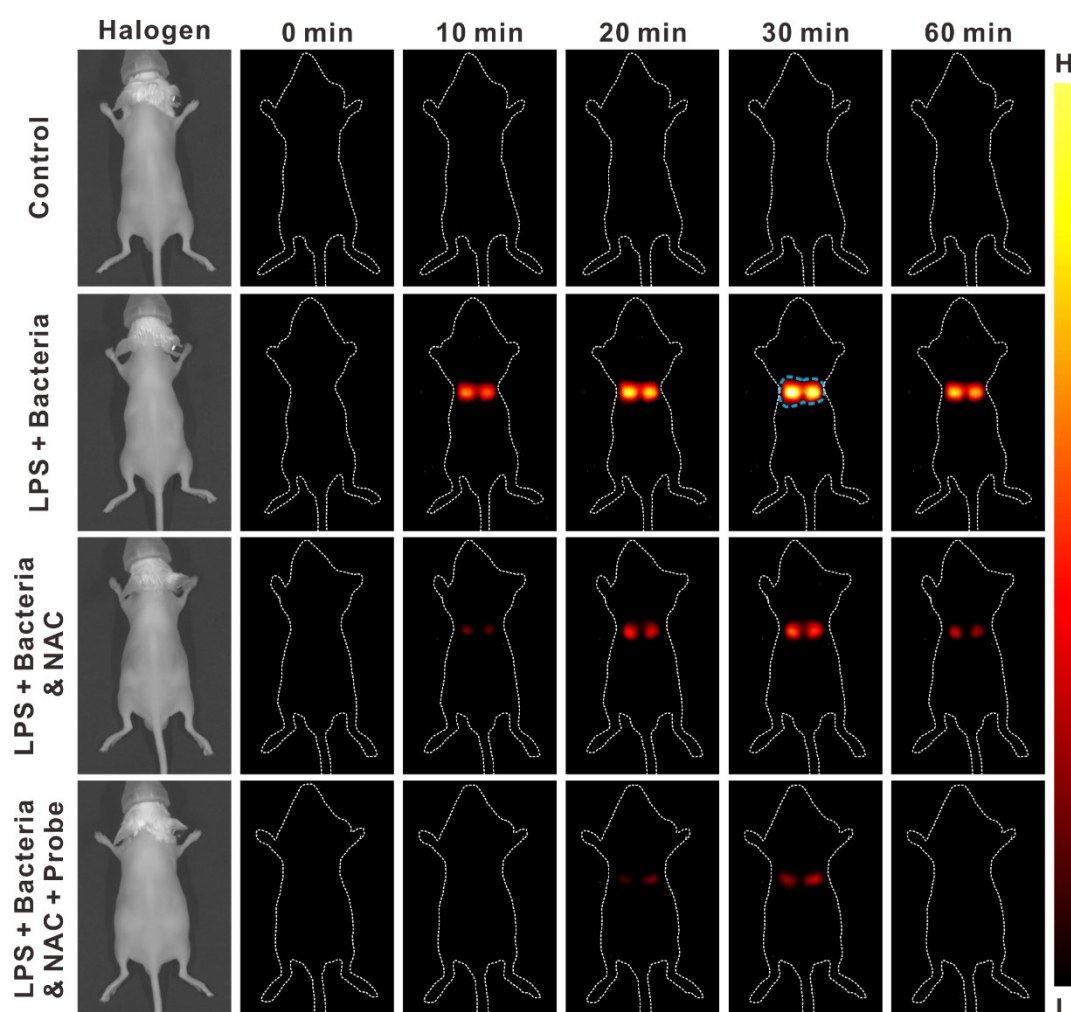


Fig. S26. Fluorescence images of the mice from different groups at different time periods after intratracheal administration of ZW-N ($0.05 \text{ mg} \cdot \text{kg}^{-1}$, in saline). The mice were in prone posture. Blue dotted circles: the ROI covering the lungs. Excitation laser: 808 nm, power density: $50 \text{ mW} \cdot \text{cm}^{-2}$.

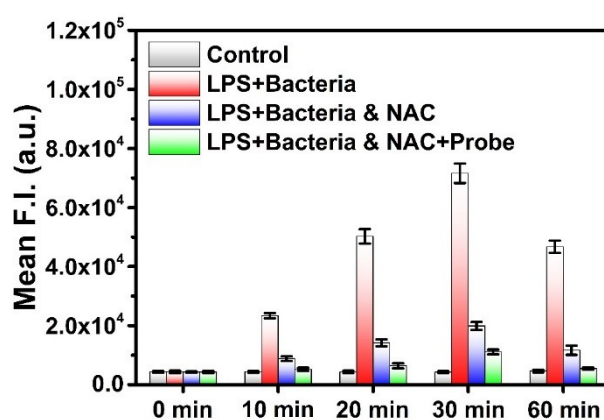


Fig. S27. Mean Fluorescent intensities at the ROI covering the lungs (Blue dotted circles) displayed in Fig. S26 ($n = 3$). Data with error bars represent the mean plus/minus SD.

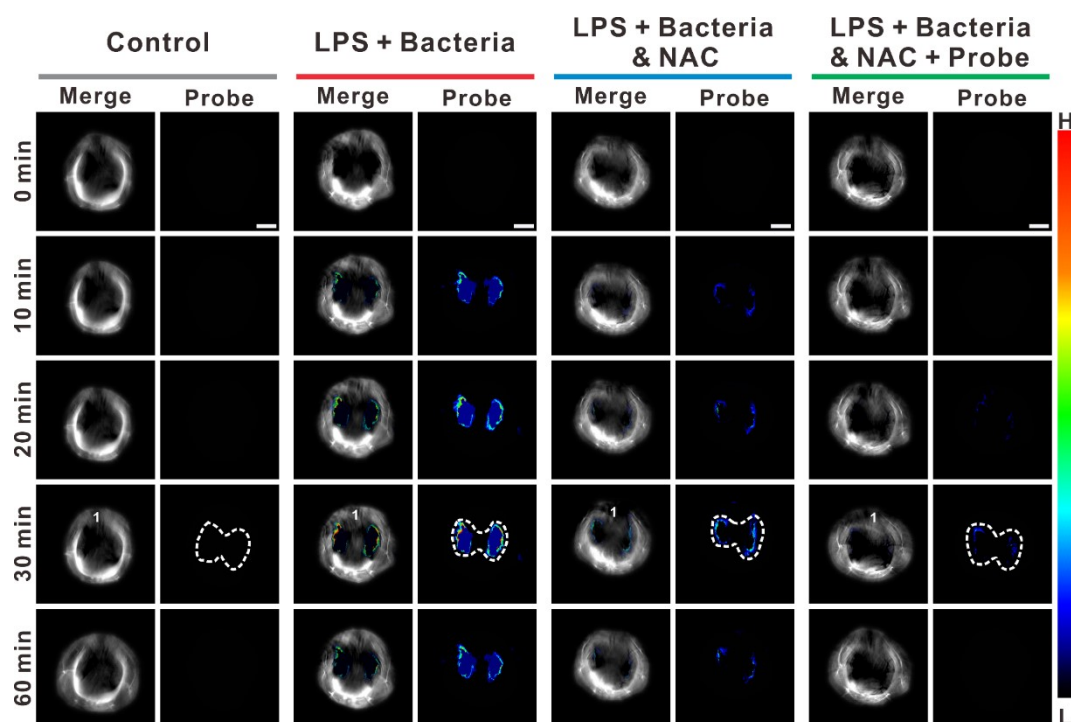


Fig. S28. Cross-sectional MSOT images of the mice from different groups at different time points after intratracheal administration of ZW-N ($0.05 \text{ mg} \cdot \text{kg}^{-1}$, in saline). Left: Overlay of the optoacoustic signals of the activated probe with the grayscale background image. Right: The optoacoustic signals of the activated probe. “1” indicates spinal cord. The mice were in prone posture. White dotted circle indicates the ROI covering the lungs. Scalebar: 5 mm.

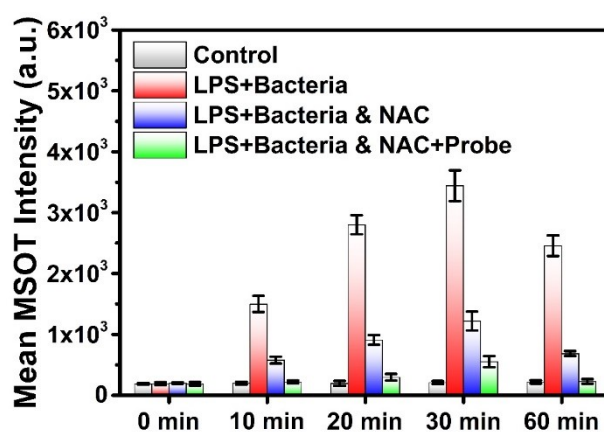


Fig. S29. Mean MSOT intensities of the ROI covering the lungs (white dotted circle) displayed in Fig. S28 ($n = 3$). Data with error bars represent the mean plus/minus SD.

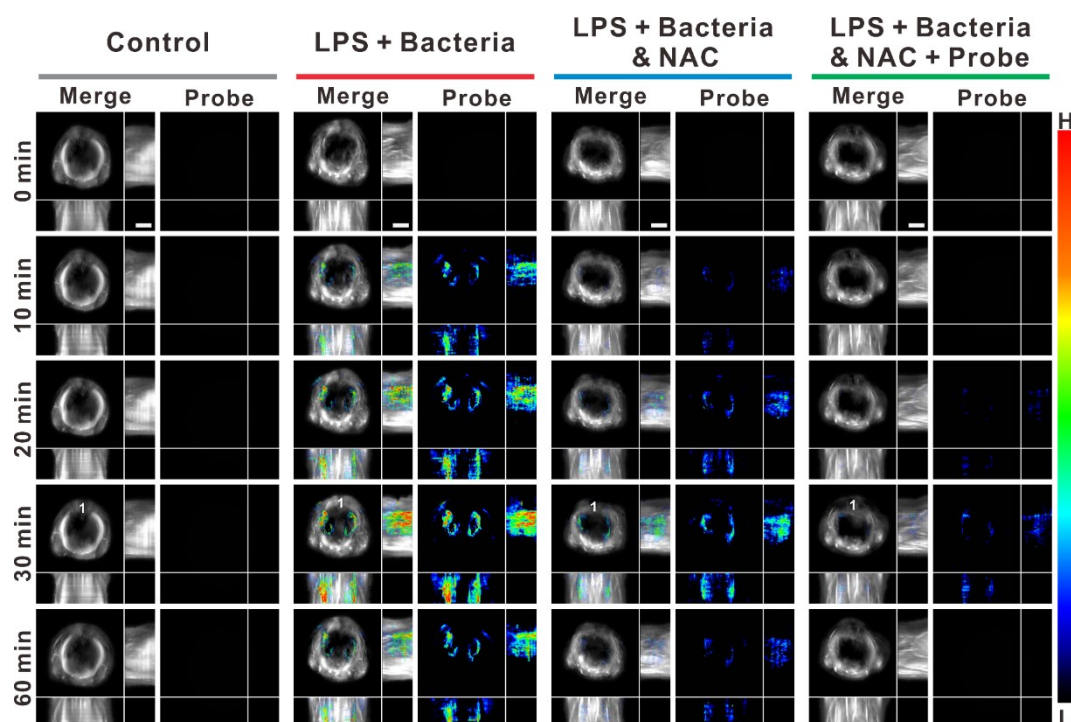


Fig. S30. 3D-MSOT images of the mice from different groups at different time points after intratracheal administration of ZW-N ($0.05 \text{ mg} \cdot \text{kg}^{-1}$, in saline). Left: Overlay of the optoacoustic signals of the activated probe with the grayscale background image. “1” indicates spinal cord. Right: The optoacoustic signals of the activated probe. The mice were in prone posture. Scalebar: 5 mm.

For the 3D MSOT images, the top-left subpanel represents the x-y plane, the top-right subpanel represents the y-z plane, and the bottom-left subpanel represents the x-z plane.

References

[S1] Z. P. She, R. Li, F. Zeng, S. Z. Wu. Homo-Dyad with Outer Hydration Layer Approach for Developing NIR-II Chromophore of High Stability and Water-Solubility as Injectable and Sprayable Optical Probe, *Adv. Healthcare Mater.* 13 (2024) 2400791.